

This document contains a post-print version of the paper

EMI Reduction for Smart Power Switches by Iterative Tracking of a Gaussian-shape Switching Transition

authored by M. Blank, T. Glück, A. Kugi, and H.-P. Kreuter

and published in *Proceedings of the International Exhibition and Conference for Power Electronics, Intelligent Motion, Renewable Energy and Energy Management (PCIM)*.

The content of this post-print version is identical to the published paper but without the publisher's final layout or copy editing. Please, scroll down for the article.

Cite this article as:

M. Blank, T. Glück, A. Kugi, and H.-P. Kreuter, "EMI reduction for smart power switches by iterative tracking of a gaussian-shape switching transition", in *Proceedings of the International Exhibition and Conference for Power Electronics, Intelligent Motion, Renewable Energy and Energy Management (PCIM)*, Nuremberg, Germany: VDE VERLAG GMBH, Berlin, 19.05.-21.05. 2015, pp. 1361–1368, ISBN: 978-3-8007-3924-0

BibTex entry:

```
@inproceedings{Blank15a,  
  author = {Blank, M. and Glück, T. and Kugi, A. and Kreuter, H.-P.},  
  title = {{EMI} Reduction for Smart Power Switches by Iterative Tracking of a Gaussian-shape Switching  
    Transition},  
  booktitle = {Proceedings of the International Exhibition and Conference for Power Electronics, Intelligent  
    Motion, Renewable Energy and Energy Management (PCIM)},  
  publisher = {VDE VERLAG GMBH, Berlin},  
  month = {19.05.-21.05.},  
  year = {2015},  
  address = {Nuremberg, Germany},  
  pages = {1361--1368},  
  isbn = {978-3-8007-3924-0}  
}
```

Link to original paper:

Read more ACIN papers or get this document:

<http://www.acin.tuwien.ac.at/literature>

Contact:

Automation and Control Institute (ACIN)
Vienna University of Technology
Gusshausstrasse 27-29/E376
1040 Vienna, Austria

Internet: www.acin.tuwien.ac.at
E-mail: office@acin.tuwien.ac.at
Phone: +43 1 58801 37601
Fax: +43 1 58801 37699

EMI Reduction for Smart Power Switches by Iterative Tracking of a Gaussian-shape Switching Transition

Mathias Blank, Tobias, Glück and Andreas Kugi
Automation and Control Institute, Vienna University of Technology, 1040 Vienna, Austria
Email: {blank, glueck, kugi}@acin.tuwien.ac.at
Hans-Peter Kreuter, Infineon Technologies Austria AG, 9500 Villach, Austria
Email: hanspeter.kreuter@infineon.com

Abstract

This paper presents a digital control strategy to track a Gaussian reference switching profile at the output voltage of a Smart Power Switch by a feedforward gate current profile. The gate current profile is adapted from switching cycle to switching cycle by an Iterative Learning Control strategy to compensate for model inaccuracies, load variations and temperature dependencies. The presented strategy reduces the generation of conducted electromagnetic interferences in a power optimal way. The strategy is verified by a series of measurement results on a rapid prototyping test bench and by an EMC compliance test according to CISPR 25.

1. Introduction

Smart Power Switches are power switches with integrated control and protection functions for the switching of middle and high current loads in industrial and automotive applications [1, 2]. In the considered case of the Smart Power Switch, the rapid switching generates conducted broadband disturbances up to 2 MHz. These electromagnetic interferences (EMI) have to be limited in order to meet the demands on electromagnetic compatibility (EMC). A common method to reduce the conducted EMI is the application of EMI-filters [3]. However, EMI-filters are bulky and cannot be integrated on the chip of the Smart Power Switch. Moreover, in particular in automotive applications the EMI filters constitute unwanted additional parts on the circuit board because they cause additional costs, space requirements and weight. Therefore, the generation of EMI has to be prevented by other measures, for instance by the active control of the switching transients [4, 3, 5].

Up to now, mostly analog control strategies are applied to control the switching transients, e.g., they control the maximum slew rate of the output voltage or the load current [6]. This slew rate limitation strategies reduce the EMI generation due to the reduction of high frequency components but also lead to an unnecessary increase of the switching losses. Since Smart Power Switches have to be operated without additional heat sinks or other cooling methods due to space and weight requirements, the switching losses are of major concern. A better trade-off between EMI reduction and occurring switching losses is achieved by the limitation of higher order derivatives [3, 5]. According to [7], a Gaussian switching profile accomplishes the optimal tradeoff between switching losses and reduction of high frequency components of the output voltage, and therefore the reduction of EMI. In [4], an analog control strategy is proposed to track a Gaussian reference transition. Analog control strategies are designed for certain load conditions and power classes and are hardly reusable for different circuit designs and applications without a major redesign.

The advent of cheap and powerful system-on-chip solutions allows to overcome these disadvantages by a digital implementation of the control strategy. A digital implementation not only reduces development costs and time to market. It also enables the application of advanced control strategies such as nonlinear and adaptive control strategies. Recently, a few digital control strategies have been presented [8, 9] and [10, 11]. In these works, adaptive gate current profiles are used to control and limit the slew rates of the switching transients. Adaptive feedforward control strategies have the potential to systematically account for dead times in the system and to compensate for model inaccuracies, temperature dependencies and load variations.

In this paper, a desired switching transition is tracked using a highly resolved adaptive gate current profile. The gate current profile is adapted by an Iterative Learning Control (ILC) strategy. Furthermore, the desired switching transition is designed by a trajectory generator depending on the supply condition of the Smart Power Switch. The presented control strategy is verified by a series of measurement results on a rapid prototyping test bench and by an EMC compliance test according to CISPR 25 [12]. The results show that the EMI can be power efficiently reduced by the proposed concept.

2. Control Strategy

For the sake of brevity only the control strategy for the switch-on operation is presented in the following. However, the strategy is applicable to the switch-off operation in the same way.

The basic idea of the control strategy is that a desired switching trajectory, e.g., a desired output voltage transition, is tracked using an adaptive feedforward gate current profile. To compensate the deviations from the desired switching trajectory, the gate current profile is adapted from switching cycle to switching cycle by an Iterative Learning Control (ILC) strategy. ILC is rewarding for systems which execute a task multiple times, see, e.g., [13, 14]. In this case, the tracking error between the desired and the actual switching transition can be minimized from one switching operation to the next. A block diagram of the proposed control strategy is depicted in Fig. 1.

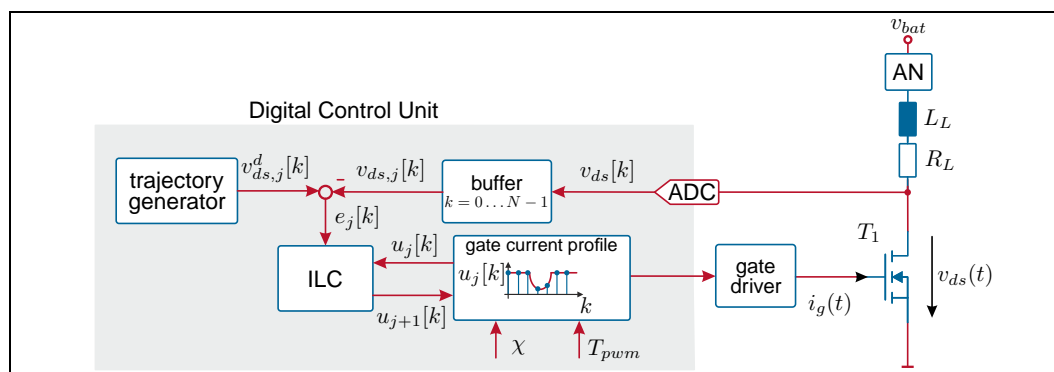


Fig. 1: Block diagram of the digital control strategy including plant and AN.

It consists of the digital control unit and the plant. The digital control unit might be a μC or an FPGA. The plant itself comprises the gate driver, the analog-to-digital converter (ADC), the

power switch T_1 and the ohmic/inductive switching load L_L and R_L . The plant is supplied with the battery voltage v_{bat} using an artificial network (AN) according to CISPR 25. The power switch operates in PWM-mode with the modulation period T_{pwm} and a duty cycle of χ . The switching operation itself is controlled by a highly resolved gate current profile, $u_j[k] = u_j(kT_s)$, where j denotes the iteration index and $k = 0, \dots, N - 1$ the sampling index. The profile is sampled with the sampling time T_s and N samples are stored in a buffer of the digital control unit. Further, $u_j[k]$ is applied to the power switch using a digitally controllable gate driver. The corresponding drain-source voltage of the power switch, $v_{ds}(t)$, is measured, sampled with T_s and N samples are also stored in a buffer, i.e., $v_{ds}[k] = v_{ds}((k + m)T_s)$. Note that the samples of v_{ds} are shifted by m in order to account for system dead times.

The trajectory generator generates the desired reference switching trajectory $v_{ds,j}^d[k]$ depending on the actual supply condition. An appropriate initial gate current profile, $u_0[k]$, can, e.g., be determined by solving an optimal control problem [15].

2.1. Iterative Learning Control Strategy

As previously mentioned, the switching operation is controlled by the gate current profile $u_j[k]$. The profile is composed of its constant maximum value u_{max} and the adaptive profile $u_{g,j}[k]$, i.e.,

$$u_{j+1}[k] = u_{max} + u_{g,j+1}[k]. \quad (1a)$$

By applying u_{max} to the gate driver, maximum switching speed and therefore minimal switching losses are achieved. Deviations from the desired switching trajectory, i.e., the tracking error

$$e_j[k] = v_{ds,j}^d[k] - v_{ds,j}[k], \quad (1b)$$

are compensated by the adaptive profile. Therefore, $u_{g,j}[k]$ is iteratively adapted from one switching operation to the next by the following ILC law

$$\bar{u}_{g,j+1}[k] = q[k] * (u_{g,j}[k] + \gamma e_j[k]), \quad (1c)$$

where $*$ denotes the discrete convolution operator, γ the constant learning gain and $q[k]$ the impulse response of the so-called Q-filter [14]. To take into account the physical limitation of the gate driver and consequently the gate current $i_g(t)$, the saturation function

$$u_{g,j+1}[k] = \text{sat}\left(\bar{u}_{g,j+1}[k], 0, -u_{max} + u_{min}\right) = \begin{cases} 0, & \bar{u}_{g,j+1}[k] > 0 \\ \bar{u}_{g,j+1}[k], & -u_{max} + u_{min} \leq \bar{u}_{g,j+1}[k] \leq 0 \\ -u_{max} + u_{min}, & \bar{u}_{g,j+1}[k] < -u_{max} + u_{min} \end{cases} \quad (1d)$$

is applied. Here, u_{min} and u_{max} are the lower and upper limit of the gate current profile, respectively. In order to avoid the learning of non-repetitive disturbances and noise, the adapted profile is filtered with the Q-filter $q[k]$. In literature, e.g., [16], a Gaussian distribution

$$g(t) = \frac{1}{\sigma_q \sqrt{2\pi}} \exp\left(-\frac{t^2}{2\sigma_q^2}\right) \quad (2)$$

with the standard derivation σ_q is often used as non causal, zero phase Q-filter. To obtain such a Q-filter, the Gaussian function (2) is discretized

$$g[k] = \frac{T_s}{\sigma_q \sqrt{2\pi}} \exp\left(-\frac{k^2}{2\sigma_q^2}\right), \quad k \in \mathbb{N} \quad (3a)$$

windowed with a rectangular window of length $2N_q + 1$ and normalized, i.e.,

$$q[k] = \frac{g[k]}{\sum_{m=-N_q}^{N_q} g[m]} \quad \text{for } k \leq |N_q|. \quad (3b)$$

The standard derivation σ_q is related to the tunable 3-dB filter bandwidth f_c by

$$\sigma_q = \frac{\sqrt{\ln(2)}}{2\pi f_c}. \quad (3c)$$

The robustness and convergence speed of the control strategy can be influenced by the learning gain γ and the 3-dB bandwidth of the Q-filter f_c . A high value of γ increases the convergence speed but decreases the robustness. Similarly, a high bandwidth f_c tends to reduce the convergence error but also weakens the robustness, see, e.g., [16, 17].

2.2. Trajectory Generator

In principle, any appropriate switching profile could be used as desired switching transition. However, according to [7], a Gaussian switching transition achieves the optimal trade-off between switching speed and reduction of high frequency components. Such a Gaussian-shape trajectory is generated by the function

$$v_{ds,j}^d[k] = \begin{cases} \bar{v}_{bat}, & k < k_s \\ \bar{v}_{bat} - v_g[k - k_s] (\bar{v}_{bat} - \bar{v}_{ds,on}), & k_s \leq k \leq k_e \\ \bar{v}_{ds,on}, & k > k_e \end{cases}. \quad (4a)$$

Herein, \bar{v}_{bat} denotes the average battery voltage, and $\bar{v}_{ds,on}$ the average on-voltage. Both voltages can either be set to an appropriate constant value or determined from the latest measurements of the drain-source voltage. Furthermore, k_s and k_e indicate the start and end index of the switching trajectory, and v_g denotes the discrete step response of the Gaussian filter kernel (3a) with $\sigma_q = \sigma_v$, i.e.,

$$v_g[k] = h[k] * g[k - k_{sw}/2]. \quad (4b)$$

Herein, $h[k]$ denotes the Heaviside function and $k_{sw} = k_e - k_s + 1$ the sampling size of the Gaussian switching trajectory. The switching trajectory starts at k_s in order to account for the turn on delay of the switching operation due to the charging of the input capacitances of the power switch.

The free design parameters of the trajectory are the truncation error of the Gaussian filter kernel (2), i.e., $\Delta_g = g(t_{sw}/2) (\bar{v}_{bat} - \bar{v}_{ds,on})$ with $t_{sw} = k_{sw}T_s$, and the maximal slew rate of the switching transient, $v_{dsp,max} = g(0) (\bar{v}_{bat} - \bar{v}_{ds,on})$. Using these parameters, the duration of the Gaussian switching profile calculates as

$$k_{sw} = \left\lceil \frac{T_s}{t_{sw}} \right\rceil = \left\lceil \frac{2}{T_s} \sigma_v \sqrt{-\ln \left(\frac{2\pi \Delta_g^2 \sigma_v^2}{(\bar{v}_{bat} - \bar{v}_{ds,on})^2} \right)} \right\rceil \quad (5)$$

with

$$\sigma_v = \frac{\bar{v}_{bat} - \bar{v}_{ds,on}}{v_{dsp,max} \sqrt{2\pi}}. \quad (6)$$

The operator $\lceil \cdot \rceil$ indicates the integer rounding towards plus infinity.

3. Rapid Prototyping Test Bench

Fig. 2 depicts the block diagram and a picture of the rapid prototyping test bench. It consists

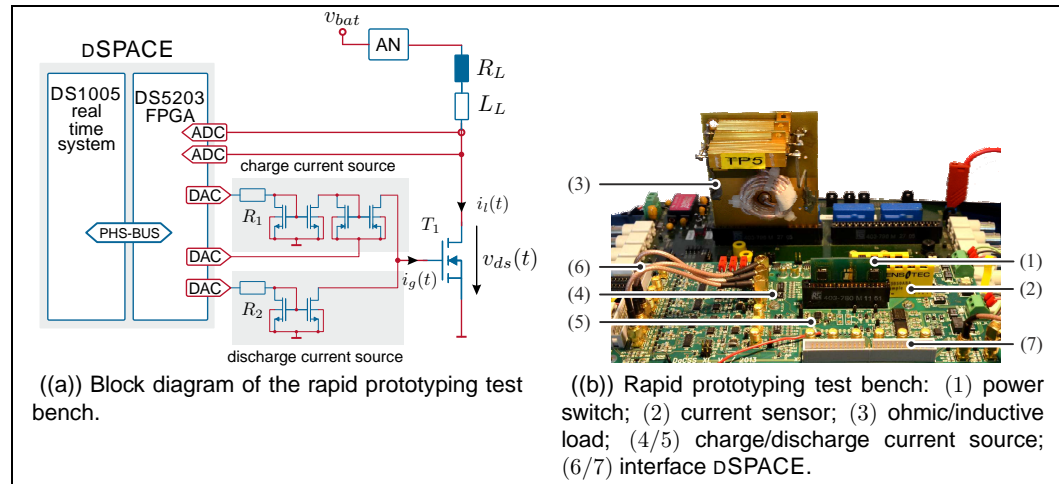


Fig. 2: Block diagram of the rapid prototyping test bench.

of the dSPACE real-time measurement and control system DS1005 PPC with the DS5203 FPGA extension board, the power switch T_1 and the ohmic/inductive switching load R_L and L_L . A digitally controllable charge and discharge current source serves as gate driver. The current sources are controlled by the 14 bit, 10 MSPS DACs of the FPGA board and provide a controllable gate current approximately in the range of ± 0.8 mA. The load current $i_L(t)$ and the drain-source voltage $v_{ds}(t)$ are first measured and then discretized by the 14 bit, 10 MSPS ADCs of the FPGA extension board. The test bench is supplied with the battery voltage v_{bat} using an artificial network (AN) according to the CSIPR 25 standard which is used to measure the conducted EMI.

4. Implementation and Measurement Results

For the following experiments, the power MOSFET BSC020N03 is used to switch a load of $R_L = 2.9 \Omega$, and $L_L = 3 \mu\text{H}$ with the battery voltage of $v_{bat} = 12.5$ V. The MOSFET is operated in PWM-mode with $T_{pwm} = 10$ ms and $\chi = 0.5$. The sampling rate of the ADC and DAC has been artificially reduced from 10 MSPS to 2 MSPS and the resolution of the ADC and DAC from 14 bit to 10 bit to simulate state-of-the-art low cost SOC hardware. Furthermore, it is assumed that the switching operation takes no longer than $100 \mu\text{s}$. Thus, the length of the gate current profile is determined to be $N = 200$.

The following EMC test results have been performed using the ESPI TEST RECIEVER from ROHDE & SCHWARZ and the artificial network NNHV 8123-200 from SCHWARZBECK.

4.1. Control Parameters

The window size of the Q-filter (3) is set to $N_q = 9$ and the 3-dB bandwidth is experimentally chosen as $f_c = 0.132$ MHz for the switch-on and switch-off operation. Furthermore, the learning

gain (1c) is set to $\gamma^{\text{on}} = -1$ and $\gamma^{\text{off}} = 1$. The system dead time is determined to be $1.5 \mu\text{s}$ and therefore the measurement vector of v_{ds} is shifted by $m = 3$. The limits of the gate current profile, see (1d), are set to $u_{\text{max}} = 9.76 \text{ V}$ and $u_{\text{min}} = 0.8 \text{ V}$ for the switch-on operation and 9.76 V and $u_{\text{min}} = 0.4 \text{ V}$ for the switch-off operation. Note that the gate current profile is in volt because the charge and discharge current sources are controlled by the output voltage of the DAC of the DSPACE system. In the experiments, the desired switching trajectories (4) are designed for different maximal slew rates with a truncation error of $\Delta_g = 10 \text{ mV/s}$ and the starting index $k_s^{\text{on}} = 4$ and $k_s^{\text{off}} = 8$.

4.2. Measurement Results

Fig. 3 ((a)) shows the time domain measurement results for the uncontrolled and controlled switching operations. The left hand side depicts the results for the turn-on operation and the right hand side for the turn-off. The gate current profiles can be found in the first row. The second row shows the drain-source voltage $v_{ds}(t)$ (solid line) together with the desired switching profile $v_{ds}^d(t)$ (dashed line). Furthermore, the control error $e = v_{ds}^d - v_{ds}$ is depicted in the third row. The last two rows show the first derivative of $v_{ds}(t)$ and $v_{ds}^d(t)$ and the time evolution of the switching losses. The maximal control error for both desired trajectories is only about 25 mV . Thus, it is evident that the presented strategy is able to track a desired switching trajectory within the given specifications. The corresponding results of the EMC compliance test can be found in Fig. 3 ((b)). The uncontrolled switching operation violates the limits of Class 4 and thus fails the Class 4 EMC test. In contrast, the EMI amplitudes of the controlled switching operations are far below the Class 5 limits and easily fulfill the highest EMC requirements. By reducing the maximal slew rate of the trajectories from $850 \text{ mV}/\mu\text{s}$ to $700 \text{ mV}/\mu\text{s}$, the spectral amplitude can only be partially lowered whereas the switching losses increase significantly. In contrast to the uncontrolled case, the controlled switching transitions exhibit a spectral peak at 2 MHz and 4 MHz . This spectral peak is a byproduct of the sampling of the gate current profile. However, the EMI level generated by the sampling frequency of the gate driver is low enough to not cause any EMI problems. However, the influence of the sampling time still has to be considered for a future circuit design so that the control circuit itself does not become the source of disturbing EMI.

5. Conclusion

In this paper, a digital control strategy was presented that tracks a desired switching trajectory at the output terminal of a Smart Power Switch. The strategy is based on an adaptive feed-forward gate current profile which is iteratively adapted by an ILC strategy in order to handle model uncertainties due to fabrication tolerances, load variations and temperature dependencies. The performance and robustness of the proposed approach were demonstrated by test bench measurements and an EMC compliance test. The measurement results show that the strategy is able to track the desired switching trajectory and to reduce the spectral amplitude of the conducted EMI far below the required levels of the CISPR 25 standard.

Acknowledgment: The authors are very grateful to Bernd Deutschmann from the Electronics Department at the TU-Graz for the help performing the EMC tests. This work was jointly funded by the Austrian Research Promotion Agency (FFG, Project No. 839316) and the Carinthian Economic Promotion Fund (KWF, contract KWF-1521 - 22741 - 34186).

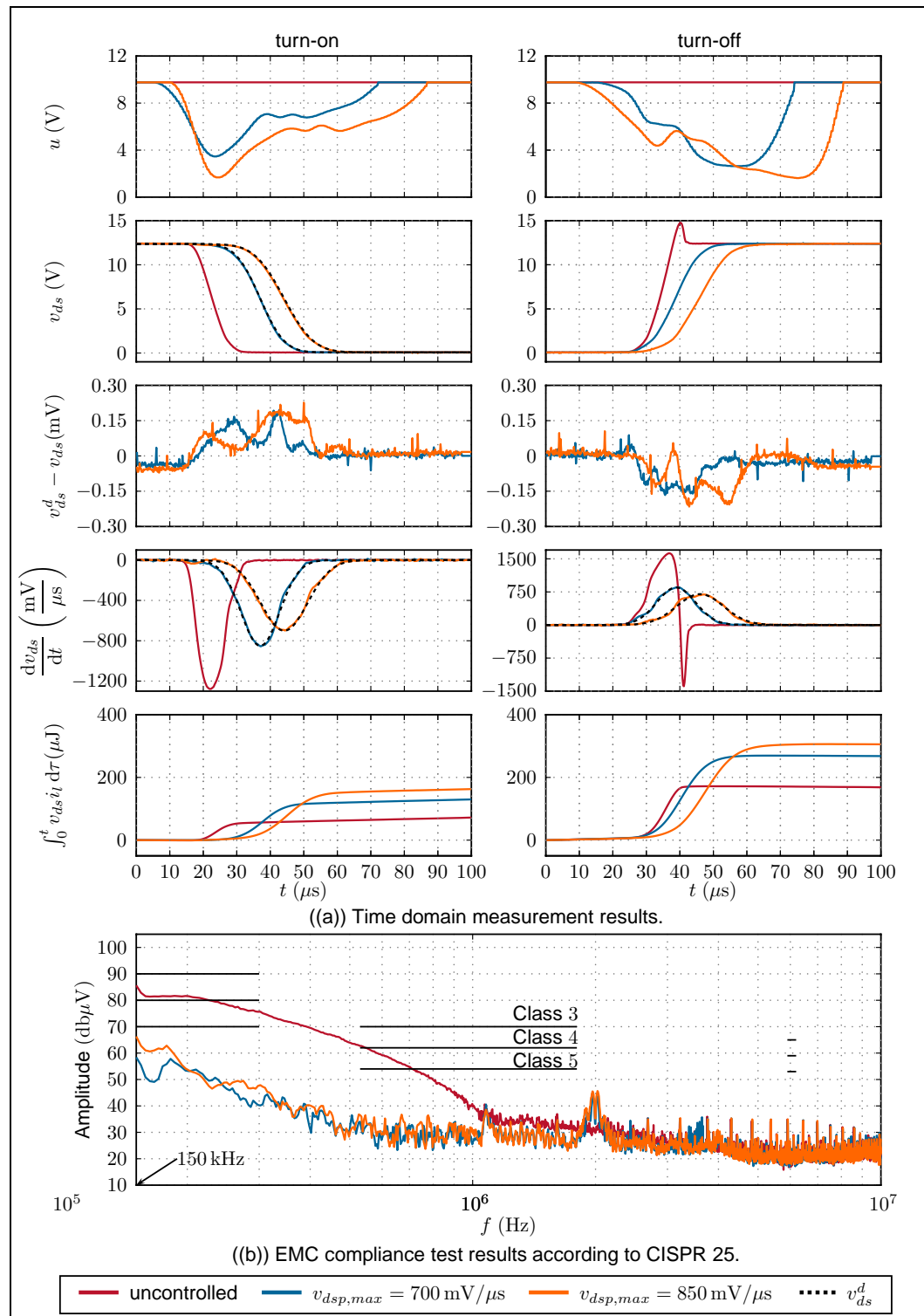


Fig. 3: Measurement results for the switching profiles with different maximal slew rates.

6. References

- [1] B. Murari, F. Bertotti, and G.A. Vignola. *Smart Power ICs: Technologies and Applications*. Springer, Berlin Heidelberg New York, 2002.
- [2] W. Pribyl. Integrated smart power circuits technology, design and application. In *Proceedings of the 22nd European Solid-State Circuits Conference, ESSCIRC '96*, pages 19–26, Neuchâtel, Swiss, 17-19 Sept. 1996.
- [3] F. Reby, R. Bausiere, B. Sohler, and F. Costa. Reduction of radiated and conducted emissions in power electronic circuits by the continuous derivative control method (cdcm). In *Proceedings of the Seventh International Conference on Power Electronics and Variable Speed Drives*, pages 158–162, London, 21-23 Sep. 1998.
- [4] X. Yang and P.R. Palmer. Shaping pulse transitions by active voltage control for reduced emi generation. In *IEEE Energy Conversion Congress and Exposition (ECCE) conference*, pages 1682–1687, Denver, 15-19 Sept. 2013.
- [5] N. Oswald, B.H. Stark, D. Holliday, C. Hargis, and B. Drury. Analysis of shaped pulse transitions in power electronic switching waveforms for reduced EMI generation. *IEEE Transactions on Industry Applications*, 47(5):2154–2165, 2011.
- [6] Y. Lobsiger and J.W. Kolar. Closed-loop IGBT gate drive featuring highly dynamic di/dt and dv/dt control. In *Proceedings of the IEEE Energy Conversion Congress and Exposition (ECCE)*, pages 4754–4761, Raleigh, NC, 15-20 Sept. 2012.
- [7] N. Patin and M.L. Vinals. Toward an optimal heisenberg's closed-loop gate drive for power mosfets. In *Proceedings of the IEEE 38th Annual Conference on Industrial Electronics Society (IECON)*, pages 828–833, Montreal, 25-28, Oct 2012.
- [8] M. Rose, J. Krupar, and H. Hauswald. Adaptive dv/dt and di/dt control for isolated gate power devices. In *Proceedings of the IEEE Energy Conversion Congress and Exposition (ECCE)*, pages 927–934, Atlanta, GA, 12-16 Sept. 2010.
- [9] L. Dang, A. Mertens, and H. Kuhn. Digital adaptive driving strategies for high-voltage igbts. *IEEE Transactions on Industry Applications*, 49(4):1628 – 1636, 2013.
- [10] M. Blank, T. Glück, A. Kugi, and H-P. Kreuter. Slew rate control strategies for Smart Power ICs based on Iterative Learning Control. In *Proceedings of the Applied Power Electronics Conference and Exposition (APEC)*, Fort Worth, 16-20 March 2014.
- [11] M. Blank, T. Glück, A. Kugi, and H.-P. Kreuter. Digital slew rate and S-shape control for Smart Power Switches to reduce emi generation. *IEEE Transactions on Power Electronics*, in press, 2015.
- [12] CISPR 25 radio disturbance characteristics for the protection of receivers used on board vehicles, boats, and on devices- limits and methods of measurement 2nd ed. IEC Std., 2002.
- [13] K.L. Moore. *Iterative learning control for deterministic systems*. Springer, London, 1993.
- [14] D.A. Bristow, M. Tharayil, and A.G. Alleyne. A survey of iterative learning control. *IEEE Control Systems Magazine*, 26(3):96–114, 2006.
- [15] M. Blank, T. Glück, A. Kugi, and H-P. Kreuter. Power optimal gate current profiles for the slew rate control of Smart Power ICs. In *Proceedings of the IFAC World Congress 2014*, pages 7190–7195, Capetown, 24-29 Aug. 2014.
- [16] D.A. Bristow and A.G. Alleyne. A high precision motion control system with application to microscale robotic deposition. *IEEE Transactions on Control Systems Technology*, 14(6):1008–1020, 2006.
- [17] Richard W. Longman. Iterative learning control and repetitive control for engineering practice. *International Journal of Control*, 73(10):930–954, 2000.